



Research article

Intestinal microbial 16S sequencing and LC-MS metabonomic analysis revealed differences between young and old cats

Tongguan Tian^{a,b}, Yuefan Zhou^{a,b}, Yixin Xu^{a,b}, Yanping Xu^{a,b,*}^a Nourse Centre for Pet Nutrition, Wuhu, 241200, China^b Shanghai Chowising Pet Products Co., Ltd, Shanghai, 201103, China

ARTICLE INFO

Keywords:

Microbial 16S
LC-MS
Metabonomic
Cats

ABSTRACT

With the progress of society, the health problems of pets have attracted more and more attention. Recent studies have shown that intestinal microflora and related fecal metabolites play a crucial role in the healthy growth of cats. However, the potential role and related metabolic characteristics of gut microbiota in different age groups of pet cats need to be further clarified. 16S rRNA gene sequencing was used to analyze the intestinal microbial composition of young and old cats. LC-MS metabonomic analysis is used to characterize the changes in the metabolic spectrum in feces. The potential relationship between intestinal microorganisms and metabolites, as well as the differences in different age groups, were studied. The species composition of intestinal microflora in the young group and old group is significantly different, T-test algorithm shows 36 different ASVs and 8 different genera, while the Wilcoxon algorithm shows 81 different ASVs and 17 different genera. The metabolomics analysis identified 537 kinds of fecal metabolites, which are rich in differences between young and old cats, and may be potential biomarkers indicating the health of cats. 16S rRNA analysis showed significant differences in fructose and mannose metabolism, while metabonomics KEGG analysis showed significant difference in choline metabolism in cancer. Our study compared the differences between the intestinal microbiome and fecal metabolites in young and old cats. This difference provides a new direction for further exploring the relationship between the composition and metabolism of intestinal microbiota in cats of different age groups. It also provides a reference for cat health research.

1. Introduction

Multiple studies have shown that genetic, environmental and dietary factors are crucial to human healthy aging and longevity [1]. With the increase of age, the ecological imbalance of intestinal flora is caused [2]. The intestinal microbiota of the elderly is significantly altered and beneficial microorganisms are reduced, suggesting that the imbalance of intestinal flora is closely related to aging. It was also reported that the imbalance of flora can lead to a series of pathological and inflammatory events [1], including changes in the level of metabolites affected by the microbiota, impairment of gastrointestinal function and integrity, which enhance systemic inflammation [3].

The human gut microbiota are a group of organisms composed of symbiotic microorganisms and co-evolve with the human body. They support the digestion and absorption of food, and metabolize it into multiple small molecules, including biologically active short-

* Corresponding author. Nourse Centre for Pet Nutrition, Wuhu, 241200, China.

E-mail address: xuyanping_nourse@163.com (Y. Xu).<https://doi.org/10.1016/j.heliyon.2023.e16417>

Received 15 February 2023; Received in revised form 11 May 2023; Accepted 17 May 2023

Available online 19 May 2023

2405-8440/© 2023 Published by Elsevier Ltd.

This is an open access article under the CC BY-NC-ND license

[\(http://creativecommons.org/licenses/by-nc-nd/4.0/\)](http://creativecommons.org/licenses/by-nc-nd/4.0/).

chain fatty acids (SCFA), which play a role in maintaining intestinal integrity, regulating host immunity, and defending against pathogens [4,5]. Intestinal microbiota, as a major regulator of immune homeostasis, promote B cells to produce various cytokines and secrete immunoglobulins to promote their own growth and inhibit pathogens by maintaining the intestinal mucus layer [6–10].

The composition of the gut microbiota was recently found to be positively associated with inflammation and longevity in the elderly [11]. The intestinal lumens of young and old people are colonized by various symbiotic microorganisms [12]. Among them, Akkermansia muciniphila, as the normal intestinal flora, is responsible for the breakdown of mucin and protection of the integrity of the intestinal barrier, thus preventing leakage and inflammation [13]. The frail elderly exhibit an increased imbalance of the gut flora, with a severe reduction of beneficial commensal bacteria and a significant increase of potentially pro-inflammatory commensal bacteria [14,15], leading to a cascade of inflammatory events that increase the incidence of age-related diseases [13,16]. Interestingly, the diversity and beneficial commensal bacteria of the microbiota of centenarians are both preserved, contributing to the control of overt inflammation and healthy aging [16].

Intestinal microflora carries out complex and active metabolic activities in the human intestine, which not only provides energy

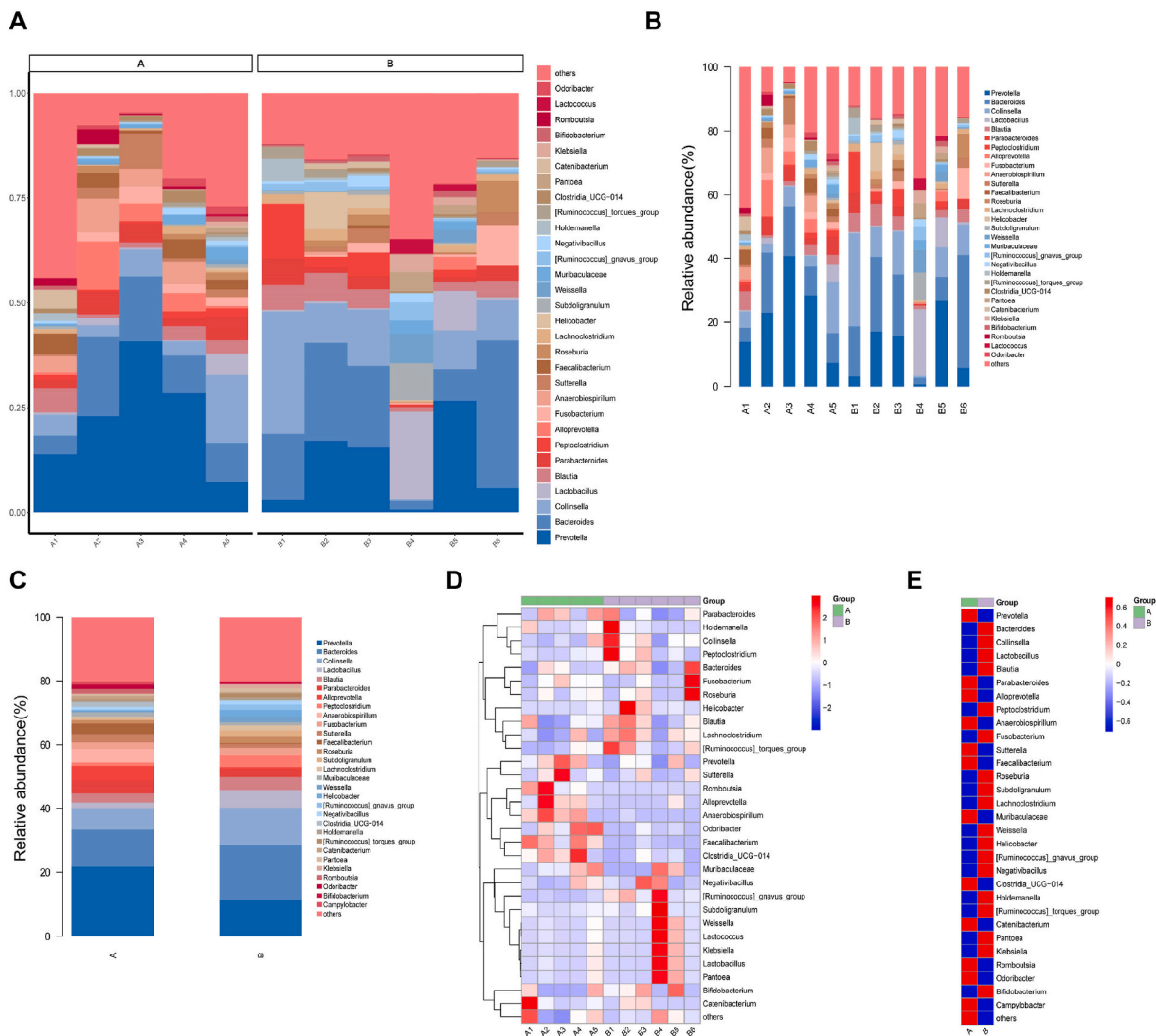
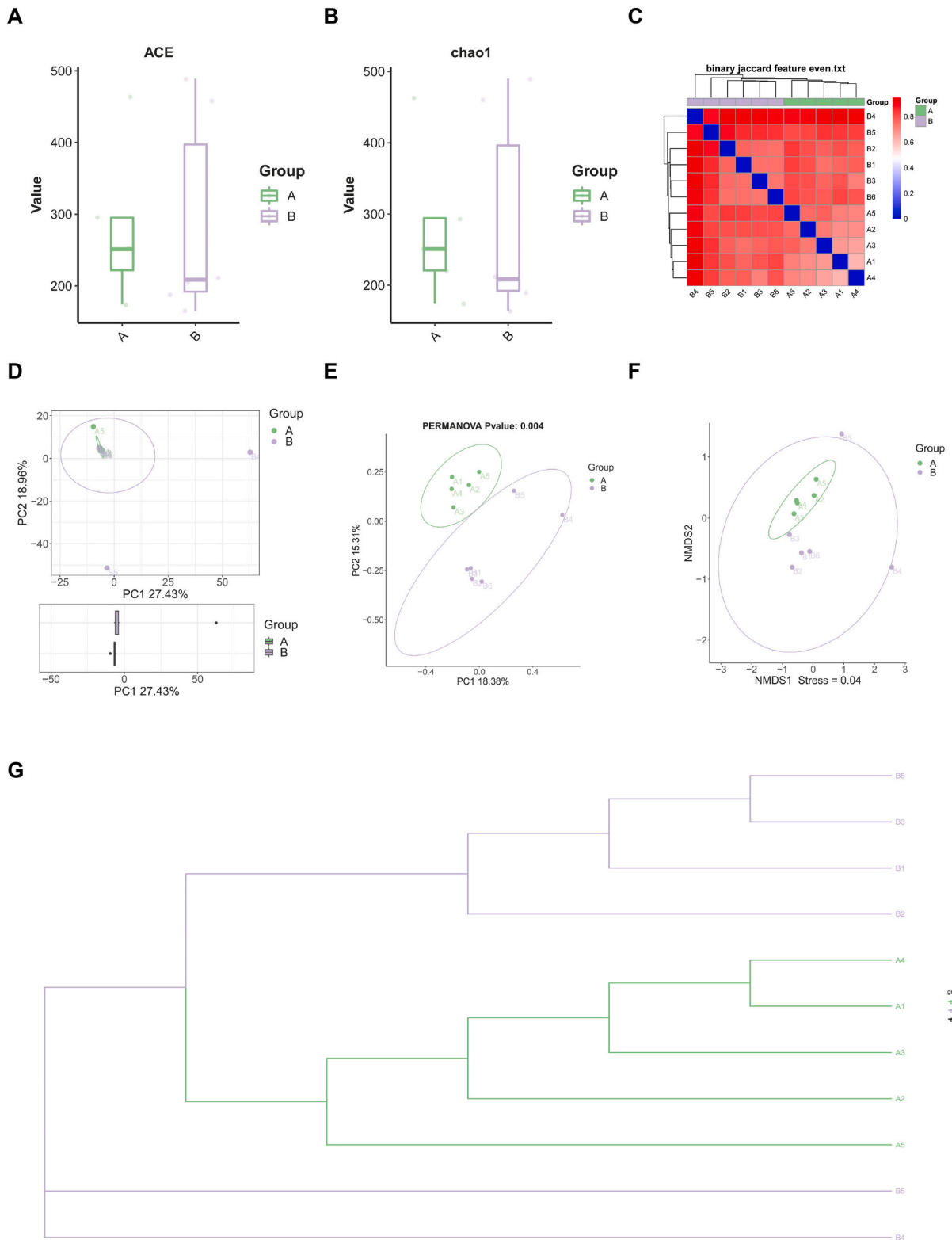


Fig. 1. Flora identification and species distribution in young and old cats (A–C) Histogram of sample community structure (shown by TOP30 as an example) The columns represent samples, different colors represent different annotation information, and others represent all species except Top. A group = Young group, B group = Aged group. (D, E) Picture description of the Heatmap map based on relative abundance. (shown by the TOP30 results of the project): The above figure shows the species abundance of TOP30 in each sample under different classification levels of the family, genus and species of the phylum. Group represents different groups, and the cluster tree on the left represents the cluster of species. The above Group represents samples from different groups. Orange indicates high relative abundance of species, while blue indicates low relative abundance of species. If the number of samples is less than 5, there is no left cluster. A group = Young group, B group = Aged group. (For interpretation of the references to color in this figure legend, the reader is referred to the Web version of this article.)



(caption on next page)

Fig. 2. Flora α/β Diversity in young and old cats

(A, B) The ASV diversity index was compared with the boxplot. Picture description: This figure shows the distribution of diversity index in each group, and whether the diversity index is significantly different between groups. The abscissa is the grouping, different groups are distinguished by different colors, and the ordinate is the index value.

(C) Sample distance heatmap diagram. Photo caption: The bluer the color is, the closer the distance between samples is, the higher the similarity is, and the redder the distance is. The samples are clustered in the heat map, and the distance relationship between samples can also be seen through the cluster tree.

(D) PCA (2D) analysis. Photo caption: The horizontal and vertical axes represent two eigenvalues that can reflect the variance to the greatest extent. Each point in the figure represents a sample, the same color is the same group, and similar samples gather together. When each group has 4 or more samples, 2D results show confidence ellipse.

(E) PCoA (2D) analysis. Picture description: The abscissa (PC1) and the ordinate (PC2) are the two main coordinates with the largest degree of interpretation of differences between samples. The same color is the same group. A point is a sample, and similar samples converge. When each group has 4 or more samples, 2D results show confidence ellipse. PERMANOVA Pvalue: 0.004.

(F) Example NMDS (2D). Picture description: abscissa (NMDS1) and ordinate (NMDS2) are two sorting axes. Each point in the figure represents a sample, and the same color is the same grouping. Similar samples gather together. If the difference between samples is large, the distance in the figure will be far. When each group has 4 or more samples, 2D results show confidence ellipse.

(G) UPGMA sample hierarchical clustering plot. A more similar sample indicates a closer branch distance. (For interpretation of the references to color in this figure legend, the reader is referred to the Web version of this article.)

and nutrients for growth and reproduction, but also produces a large number of metabolites in human body [17,18]. By comparing the metabolites in the blood of sterile animals and bacteria animals, it was found that hundreds of metabolites were detected only in bacterial mice [19]. Undigested food (mainly including protein, carbohydrate, etc.) is the main metabolic substrate of intestinal flora, which can be metabolized by intestinal flora after reaching the gastrointestinal tract and produce multiple bacterial metabolites, such as lipopolysaccharide, peptidoglycan, trimethylamine, secondary bile acid and SCFA, thus causing different effects on human health [20–23].

This study mainly analyzes and compares the differences in intestinal microorganisms and metabolites between young and old cats, to determine the possible relationship between different microbial genera and related metabolites in different age groups, and further determine which microbial genera and metabolites play a role in aging, thus guiding the healthy diet of cats.

2. Results

2.1. Flora identification and species distribution in young and old cats

Based on microbial diversity and 16S rRNA gene sequence identity, we identified 31 genera of intestinal flora in two groups of cats (Fig. 1). The analysis of microbial components showed that in the elderly group, Prevotella, Paraacteroides, Alloprevotella, Anaerobiospirillum, Sutterella, Faecalibacterium, Muriaculaceae, Clostridia, Catenibacterium, Romboussia, Odoribacter, and Campylobacter Fungi are abundant (Fig. 1A–E). In the young group, Bacteroides, Collinella, Lactobacillus, Blautia, Peptoclostridium, Fusobacterium, Roseburia, Subdoligranum, Lachnochlostridium, Weissella, Helicobacter, Ruminococcus_gnavus_group, Negativibacillus, Holdemanna, Ruminococcus_torques_group, Pantoea, Klebsiella and Bifidobacterium are abundant (Fig. 1A–E). Compared with the two groups, the two genera of Prevotella and Paraacteroides in the young group are the dominant flora, while in the elderly group, Bacteroides and Collins are the dominant flora (Fig. 1A–E).

2.2. Flora α/β diversity in young and old cats

α Differences in diversity, including ACE (Fig. 2A) and Chao1 (Fig. 2B) indexes, were evaluated by Mann-Whitney *U* test. Compared with the young group and the old group, the ACE and Chao1 indexes of the young group were higher than those of the old group. The beta diversity index shows that the distance between sample branches can be seen by hierarchical clustering of the matrix according to the distance matrix obtained by different distance algorithms. It shows that the young group is far away from the old group and the similarity is low (Fig. 2C). PCA analysis is expressed by variance decomposition. The more similar the composition between samples, the closer the distance reflected in the PCA diagram (Fig. 2C, D). Therefore, PCA analysis indicates that the two groups of samples have a certain degree of similarity. PCoA analysis shows that the two groups of samples have high similarity within the young group, while two samples in the old group are far away, and the similarity within the sample group was low, while the comparison between groups had certain differences (Fig. 2E). The results of NMDS analysis are similar to those of PcoA analysis (Fig. 2E, F). In addition, the results of sample hierarchical cluster analysis showed that the differences within the young group were small, while the differences within the older group were large (Fig. 2G). Together, the results of the two groups showed that the diversity of the older group was smaller than that of the younger group.

2.3. LEfSe analysis identified the greatest difference between young and old cats

LEfSe (Linear Discriminant Analysis Effect Size), also known as LDA-Effect Size analysis, is an analytical tool that discovers and interprets high-latitude data biomarkers. It can enable comparisons between two or more groups, as well as comparative analysis

between subgroups within the same group, to identify species with significant differences in abundance between groups. We used the cut-off value of 2.0 logarithmic LDA score to determine the important classification differences between the young group and the old group, and found that there was a significant difference in the fecal microbial population between the young group and the old group derived from the LDA-LefSe analysis (Fig. 3A). We found that the relative abundance of Bacteria in the young group was lower than that in the old group, while the relative abundance of Ruminococcus, Butyricimonas, Lachnospiraceae and Bilophila in the old group was higher than that in the young group (Fig. 3A and B). As shown in Fig. 3C–H, compared with the young group, the average abundance of Ruminococcus and Butyricimonas in the elderly group increased significantly (Fig. 3C and D). On the contrary, the

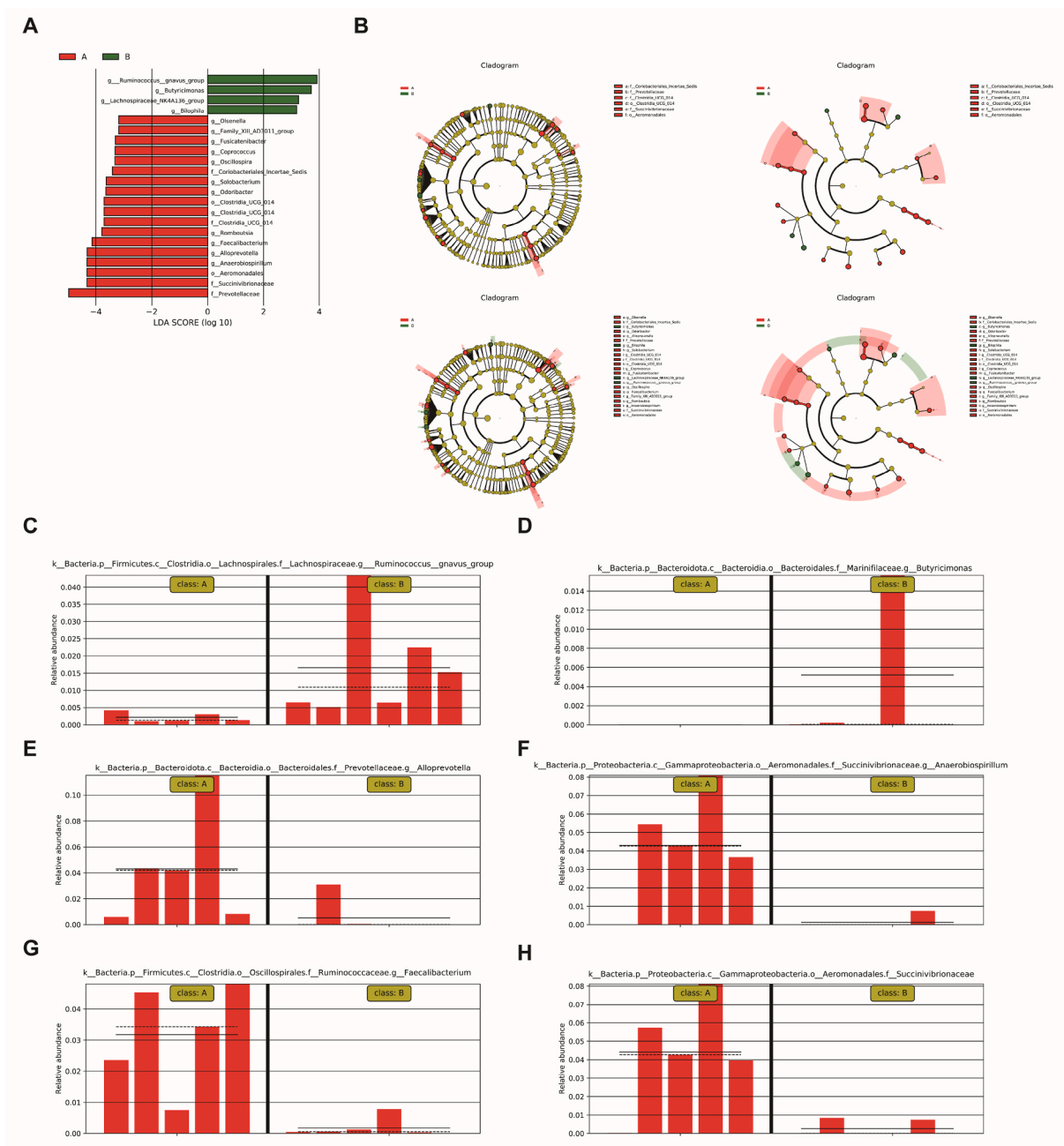


Fig. 3. LefSe analysis identified the greatest difference between young and old cats (A) Linear discriminant analysis (LDA) effect size (lelse) analysis showed significant bacterial differences in fecal microbiota between the elderly group (positive score) and the young group (negative score). (B) Cladogram using the lelse method indicating the phylogenetic distribution of fecal microbiota associated with the young and old groups. (C–H) The relative abundance of Ruminococcus (C) ($P = 0.0062$), Butyricimonas (D) ($P = 0.0345$), Prevotellaceae (E) ($P = 0.0176$), Succinivibrionaceae (F) ($P = 0.0151$), Faecalibacterium (G) ($P = 0.0106$) and Aeromonadales (H) ($P = 0.0166$). Solid and dashed lines indicate mean and median, respectively.

average abundance of Prevotellaceae, Succinivibrionaceae, Faecalibacterium and Aeromonadales in the young group increased significantly (Fig. 3E–H). Taken together, compared to the younger group, the other genera in the elderly group are more abundant, but the absolute difference between the two groups is less than the difference observed by Bacteria.

2.4. KEGG pathway prediction of metagenome functional content from 16S rRNA

OTU abundance is standardized by using the 16S rRNA gene copy number identified by the green gene database, and the homology prediction of the Kyoto gene and genome encyclopedia (KEGG) is calculated (Fig. 4A and B). Compared with the young group, 6 of the 30 KEGG metabolic pathways analyzed were enriched to varying degrees in the elderly group (Fig. 4C). Compared with the young group, all six significantly different pathways in the old group were exhausted. In the elderly group, the consumption of the KEGG pathway of fructose and mannose metabolism was the most significant (both P = 0.03) (Fig. 4C). A recent genome-wide and transcriptomic study showed that there was a correlation between plasma mannose, body mass index, and insulin resistance, and mannose could help intestinal flora resist the harmful effects of obesity induced by a high-fat diet. Bacteria can sense their environment and change the expression of proteins to improve their viability. The above results show that with the growth of age, the intestinal flora of the body will accelerate the metabolism of mannose to keep the body healthy.

2.5. Choline and tomatidine in the elderly group were significantly lower than those in the young group

In order to study the fecal metabolite levels of cats of different age groups, liquid chromatography-tandem mass spectrometry (LC-MS) was used to evaluate the metabolites of old and young cats, and univariate analysis was used for analysis. Through gene peak map analysis (Fig. 5A) the results show that there is no significant difference between the two groups of samples in the initial quality control analysis. Principal component analysis (PCA) (Fig. 5B) with no quality control and orthogonal partial least squares discriminant

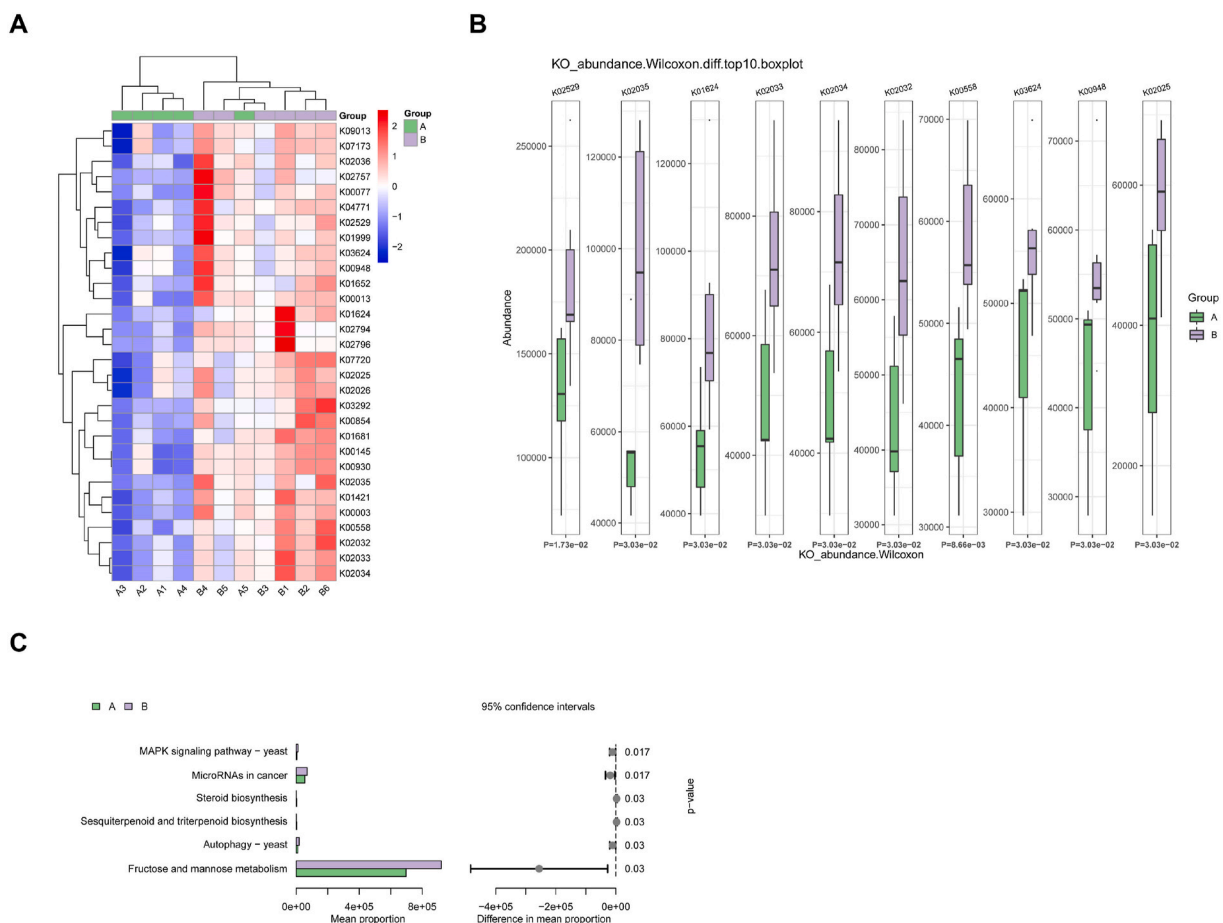


Fig. 4. KEGG pathway prediction of metagenome functional content from 16S rRNA (A) KEGG differential outcome clustering Heatmap plot. (B) KEGG differential results boxplot plot. (C) KEGG differential outcome bar chart, with the left bar representing the mean abundance of a pathway in each group and the right 95% confidence interval of the differential contrast between the groups along with the corresponding p value for significance.

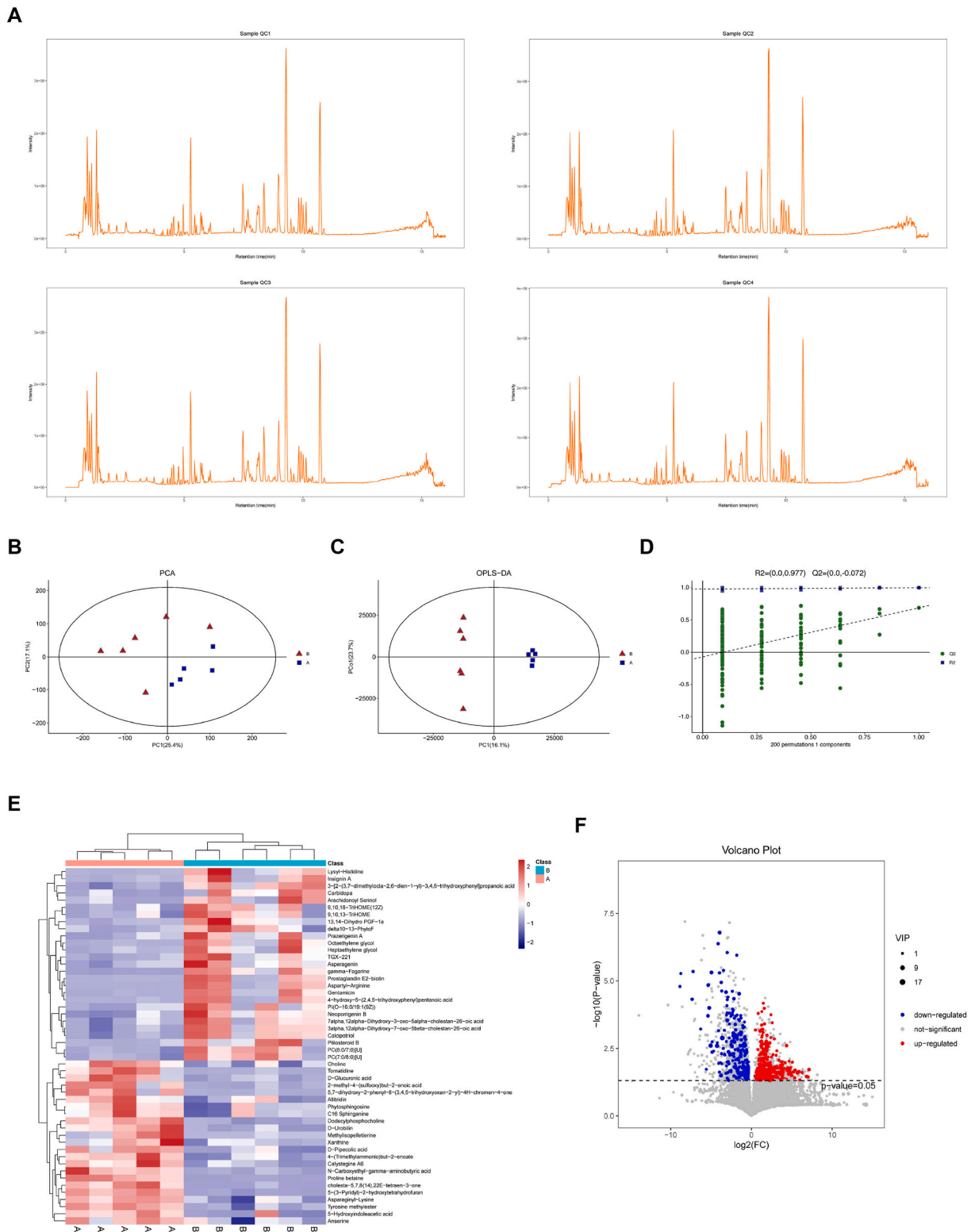


Fig. 5. The difference of fecal metabolites between the two groups. (A) Gene peak map shows that there are few abnormal cases in the sample. (B) PCA scores shows that the sample has good stability and repeatability. (C, D) Multivariate statistical analysis show that the sample aggregation is good. (E) Two-way hierarchical clustering heatmap of fecal metabolome data. Each column shows the metabolic pattern of individual animals in the A group (n = 5) and B group (n = 6). (F) Volcano plot showing metabolites for A and B group.

analysis (OPLS-DA) (Fig. 5C and D) were used to validate differences between these two groups. Further evaluation of the two groups of data indicates that the samples are relatively independent in two groups, and there is no obvious crossover. MetaboAnalyst 4.0 software was used to generate a heat map containing 50 kinds of metabolite dendrograms, to intuitively determine the changes in metabolite levels between the old group and the young group (Fig. 5E). To better provide proper nutrition components for cat food, to be more beneficial to the survival of elderly cats, we analyzed the metabolite in the feces of the elderly group, and found that 23 kinds of metabolite showed a decline, respectively: Choline, Tomatidine, D-Glucuronic acid, 2-methyl-4-(sulfooxy)but-2-enoic acid, 5,7-dihydroxy-2-phenyl-8-(3,4,5-trihydroxyoxan-2-yl)-4H-chromen-4-one, Allitridin, Phytosphingosine, C16 Sphinganine, Dodecylphosphocholine, D-Urobinin, Methylisopelletierine, Xanthine, D-Pipecolic acid, 4-(Trimethylammonio)but-2-enoate, Calystegine A6, N-Carboxyethyl-gamma-aminobutyric acid, Proline betaine, cholesta-5,7,8(14),22E-tetraen-3-one, 5-(3-Pyridyl)-2-hydroxytetrahydrofuran, Asparaginyl-Lysine, Tyrosine methylester, 5-Hydroxyindoleacetic acid, Anserine. Fig. 3E lists all the differences in metabolite screening, and was further illustrated in the form of a volcano plot (Fig. 5F). As shown in the final screening result, the significant up-regulation of the metabolites was displayed in red, while the significant down-regulation of the metabolites was shown in blue.

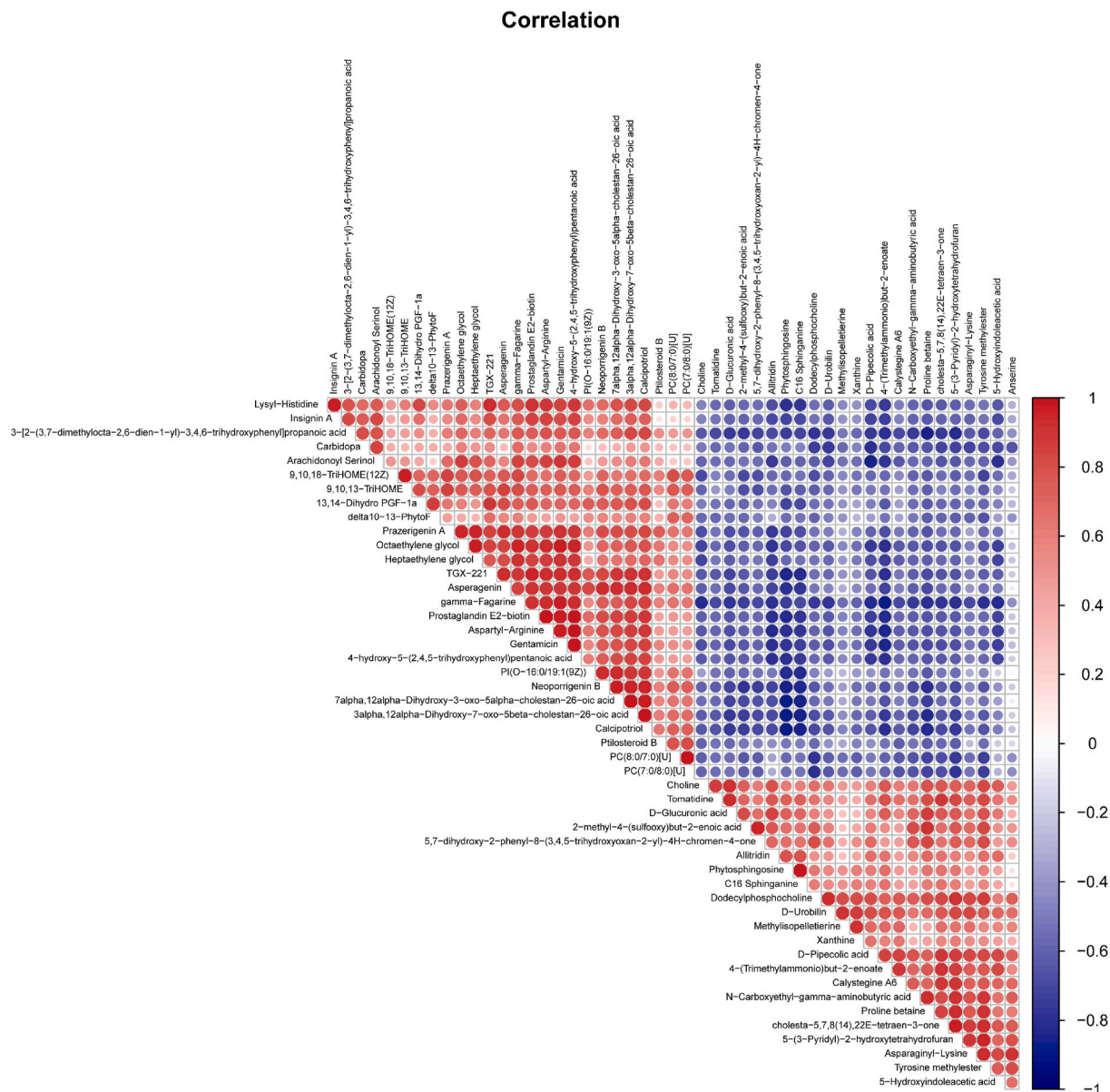


Fig. 6. Metabolites-metabolites correlation analysis. Metabolites-metabolites correlation analysis. Positive correlations are shown in red; negative correlations are shown in blue. Metabolites-metabolites correlations of A group vs. B group. (For interpretation of the references to color in this figure legend, the reader is referred to the Web version of this article.)

2.6. Metabolites-metabolites correlation analysis

The correlation value matrix provides a more intuitive description of the relationship between related metabolites (Fig. 6). Metabolites with a high positive correlation of Choline mainly include Tomatidine, Proline betaine, 5-hydroxy indole acetic acid, Allitridin, 4-(Trimethylammonio) but-2-enoate. Taken together, choline and tomatidine were lower in the elderly group, and they were positively correlated.

2.7. Analysis of KEGG pathway shows that choline metabolism is significant in cancer

By analyzing and comparing relevant metabolic enzymes and metabolites, we identified the metabolic pathways that underwent changes. In addition, KEGG analysis was used to identify the enriched metabolites (Fig. 7). The results showed that following four metabolic pathways were mainly enriched in the elderly group: choline metabolism in cancer, glycerophospholipid metabolism, retrograde endocannabinoid signaling and linoleic acid metabolism, respectively (Fig. 7A and B). Together, KEGG analysis showed that choline metabolism is the most significant in cancer, indicating that choline loss may be related to cancer occurrence.

3. Discussion

Intestinal microorganisms play important roles in host physiology, pathology, and intestinal immune balance. In the present study, two genera of Prevotella and Parabacteroides served as the dominant flora in the young group. While in the elderly group, two genera, Bacteroides and Collinsella, served as the dominant flora. However, with increasing age, 16S sequencing found that fructose and mannose metabolism was more vigorous in the aged group, possibly due to organismal aging, and the gut flora accelerated this metabolism to maintain organismal health to resist aging. Meanwhile, the changes of intestinal metabolites in different age groups were also analyzed in this study, and choline, as a product of weakened metabolism in the aged group, predicts that the decrease of choline level may be related to aging, so the appropriate supplementation of choline may slow down aging.

Intestinal dysbiosis in the elderly increases the risk of aging-related diseases [24]. The composition of the intestinal flora changes with age, and this change is exacerbated by changes in antibiotic intake and diet [25]. A report on the sequencing of human fecal microbiota showed that the microbial composition of the gastrointestinal tract is influenced by many factors, such as individual differences, environmental changes, and lifestyle [26]. In people with morbid obesity [27], there is a shift in the intestinal flora from a protective flora to a damaging flora. Similarly, similar changes of microbiota occur during aging and may be due to various pathologies and diseases [28–35]. Recent results of microbiota sequencing in Chinese elderly suggest that changes in the microbiota may be an intrinsic factor in the process of aging [36].

Intestinal microbiota is an endogenous ecosystem composed of bacteria, archaea, eukaryotes and viruses, in which Firmicutes, Bacteroidetes, Proteobacteria and Actinobacteria account for 98% of the microbial population. Microbial colonization in the gastrointestinal tract after birth begins with the acquisition of several microbial types dominated by bifidobacteria. In the early stage, the infant microbiota is unstable, as its microbial colonization can be affected by many factors [37]. With age, the gut microbiota stabilizes and exhibits a diverse flora, including a mixture of 11 bifidobacteria and lactobacilli [38]. In adulthood, the intestinal microbiota is dominated by Firmicutes and Bacteroidetes, with less Actinobacteria and Proteobacteria [38]. Notably, a previous sequencing analysis of the human fecal metagenome demonstrated that diet is a major driver of changes in microbial composition and function [39].

SCFA is produced by a number of bacteria groups that work in concert with the commensal flora and function accordingly. Butyrate

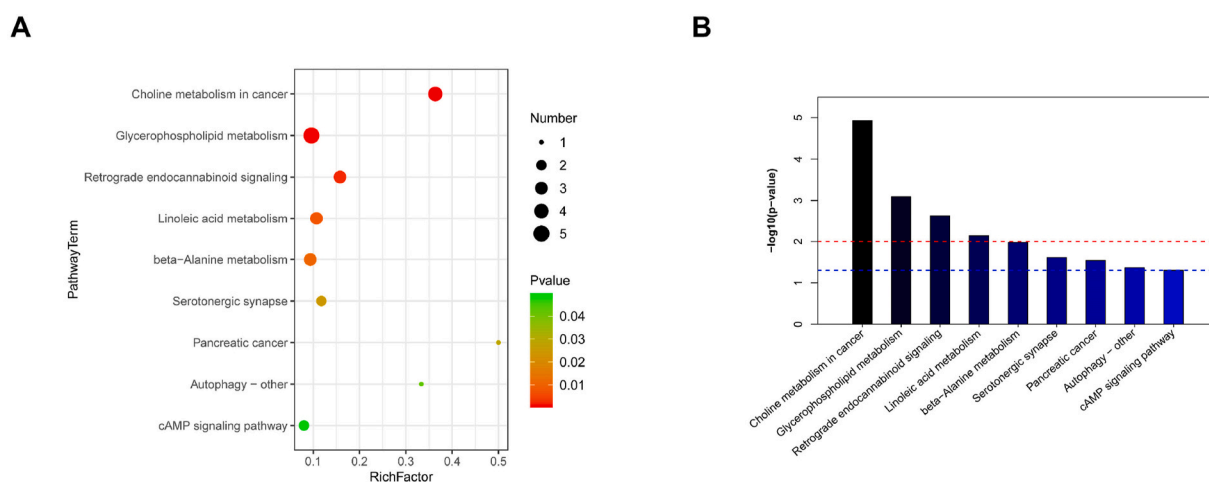


Fig. 7. Analysis of KEGG pathway shows that choline metabolism is significant in cancer. (A–B) KEGG enrichment analysis of the differentially abundant metabolites in A group vs. B group. KEGG significantly enriched Top10.

plays an important role in epithelial homeostasis by activating the oxygen sensor hypoxia-inducible factor, protecting intestinal integrity, and inhibiting inflammation and adverse immune responses in intestinal tissues [40]. In the elderly, SCFA levels from carbohydrate fermentation decreased while metabolic products from protein fermentation (branched-chain fatty acids, ammonia, and phenols) increased, indicating a shift in glycolytic fermentation toward unfavorable proteolytic activity [41]. Multiple studies have shown that regulating intestinal flora by supplementing probiotics, prebiotics and transplanting intestinal flora can increase intestinal microbial diversity and produce benign metabolites, improving intestinal microenvironment, alleviating inflammation, and hopefully achieving the purpose of delaying aging [42–44].

The intestinal flora in animals is large in number and complex in type, forming a symbiotic relationship with the body that is "mutually beneficial". Their growth depends on abundant nutrients and a relatively safe environment provided by their bodies. At the same time, they play a crucial role in maintaining physical health and promoting normal development. At present, the researches on adding probiotics or metabolites to cat food mainly focus on the addition of some conventional probiotics and metabolites. For example, the microbiota includes *Bacillus* and *Lactobacillus*, while metabolites include choline. The addition of these probiotics and metabolites is bound to change the animal's own intestinal flora and metabolic mode, because the reasonable addition of the corresponding probiotics and metabolites is the direction of the future development of cat food, and it is certain that the addition of these probiotics and metabolites will improve the quality of life of pet cats.

In conclusion, by comparing the gut flora genera of old and young cats with fecal metabolites, choline was found to be significantly decreased in old cats, while KEGG showed that choline metabolism was associated with cancer. Meanwhile, it was found that the dominant genera of gut microbiota in different age groups had some differences. Whether these differences are the main reasons for the differences in metabolites, or the differences in metabolites are caused by the differences in intestinal microflora? Further studies are needed to identify the relationship between gut microbiota and metabolites during cat aging.

4. Materials and methods

4.1. Chemicals

All chemicals and solvents were analytical or HPLC grade. Water, methanol, acetonitrile, formic acid were purchased from Thermo Fisher Scientific (Thermo Fisher Scientific, Waltham, MA, USA). L -2-chlorophenylalanine was from Shanghai Heng chuang Biotechnology Co., Ltd. (Shanghai, China).

4.2. Cats information and sample preparation

Cats were collected from Nourse Centre for Pet Nutrition, Wuhu, China. The basic information of cats is shown in Table 1. Cats age stage classification refers to the 2021 AAHA/AAFP Feline Life Stage Guidelines. The stool sample collection procedure was as follows: After fasting the cat and treating it with water for 24 h and perianal disinfection, the cat was urged to defecate by abdominal massage. Then, 300–500 mg feces were collected with sterile forceps and stored in sterile cryopreservation tubes at -80°C for subsequent fecal DNA extraction and bacterial flora testing.

4.3. Fecal DNA extraction

Each stool sample (200 mg) was aseptically weighed and transferred to a 2 mL Ep tube. Then, fecal DNA was extracted using the PowerSoil DNA Isolation Kit (MoBio Laboratories, Carlsbad, CA), and DNA quality and concentration were assessed using the Nano Drop fluorescence spectrometer.

4.4. Library construction and high-throughput sequencing

Libraries were constructed with a library construction kit and quantified using a Qubit instrument and qPCR. Then, after the MiSeq

Table 1
Basic information of cats.

Groups		Weight (Kg)	Age (year)	Gender
A	A1	4.2	2.7	Female
	A2	4.6	2.6	Female
	A3	6.3	2.4	Male
	A4	5.6	2.4	Male
	A5	4.8	2.3	Female
B	B1	5.1	11.4	Female
	B2	5.3	12.1	Female
	B3	7.1	18.6	Female
	B4	5.2	9.2	Male
	B5	5.3	9.7	Female
	B6	6.1	13.4	Male

library passed the quality check, 16S rRNA gene V3–V4 sequencing was performed on the Illumina MiSeq platform.

4.5. Sequence analysis

After downloading the raw sequencing data, a quality control step was performed to obtain the optimized sequence through sequence splicing, filtering, and de-chimizing. Operational taxonomic units (OTUs) were then clustered and annotated with a similarity threshold of 97%. The results of alpha diversity analysis included alpha diversity index dilution curve, alpha diversity index violinplot analysis, Specaccum species accumulation curve and Rank Abundance analysis. Beta diversity analysis provides: (1) Distance matrix analysis, PCA, PCoA, NMDS, UPGMA analysis (2) To test whether there is a significant difference between the two comparison groups: Adonis analysis (i.e. PERMANOVA analysis) and Anosim analysis.

4.6. Sample preparation for global metabolomics

About 60 mg of the frozen intestinal contents sample was added to a 1.5 mL EP tube with 20 μ L of L-2-chlorophenylalanine (0.06 mg/mL) dissolved in 600 μ L methanol-water (V: V = 4:1) as internal standard, and the tube was added two small steel balls. Subsequently, the tube was placed in a refrigerator at -20°C for 5 min, and then grinded in a grinder (60 Hz, 2 min), and the whole samples were extracted by ultrasonic for 10 min in ice-water bath, stored at -20°C for 30 min. The extract was centrifuged for 10 min (13000 rpm, 4°C). 200 μ L of the supernatant was transferred to an LC-MS vial and evaporated to dryness. 300 μ L of methanol-water (V: V = 1:4) (vortexed for 30 s, sonicated for 3 min), then standed at -20°C for 2 h. Samples were centrifuged for 10 min (13000 rpm, 4°C). 150 μ L of the supernatant were aspirated with a syringe, filtered with a 0.22 μ m organic phase pinhole filter, transferred to an LC injection vial. The vials were stored at -80°C until LC-MS analysis. Quality control samples (QC) are prepared by mixing equal volumes of extracts from all samples.

4.7. Liquid chromatography-mass spectrometry analysis conditions

The analytical instrument used in this experiment is a liquid mass spectrometry system composed of ACQUITY UPLC I-Class plus ultra high performance liquid chromatography in series with QE plus high-resolution mass spectrometer.

Chromatographic conditions: Chromatographic column: ACQUITY UPLC HSS T3 (100 mm \times 2.1 mm, 1.8 μ m); Column temperature: 45°C ; Mobile phase: A-water (containing 0.1% formic acid), B-acetonitrile (containing 0.1% formic acid); Flow rate: 0.35 mL/min; Injection volume: 2 μ L.

4.8. Statistical methods

Illumina MiSeq or NovaSeq sequencing generates raw double-ended sequences called raw data. Using cutadapt software, cut out the primer sequence from the raw data sequence. Use DADA2 to perform quality control analysis such as quality filtering, noise reduction, splicing and chimera removal on the qualified double-ended raw data in the previous step with Qiime2 default parameters to obtain the representative sequence and ASV abundance. At each classification level, the OTU barplot statistics of the number of OTUs and annotation results of each sample were carried out, and the clean tags, valid tags, tags with annotation information and OTUs of each sample were compared. Microbial multivariate statistical analysis to test whether there is a significant difference between the two groups: (1) Routine: T test algorithm, Wilcoxon algorithm, for the significance analysis of the difference between the two samples, Metastat analysis method was used; (2) LEfSe analysis (provided when the number of groups is less than or equal to 6), combined with difference detection method (Kruskal Wallis test or Wilcoxon test) and linear discriminant analysis method for feature selection.

Multivariate statistical analysis will first use unsupervised principal component analysis (PCA) to observe the overall distribution of each sample and the stability of the whole analysis process, and then use supervised partial least squares analysis (PLS-da) and orthogonal partial least squares analysis (OPLS-da) to distinguish the overall differences of metabolic profiles between groups and find the different metabolites between groups. Univariate analysis mainly focuses on the description of univariate and statistical inference, which reflects the basic information contained in a large number of sample data in the simplest form and describes the concentration or dispersion trend of sample data. Univariate statistical inference is to infer the overall situation from sample data, mainly including interval estimation and statistical hypothesis testing. T-test (Student's *t*-test) and fold variation analysis (Fold change analysis) were often used to compare metabolites between the two groups. Multidimensional analysis and unidimensional analysis were used to screen the different metabolites between groups. In OPLS-da analysis, Variable important in projection (VIP) can be used to measure the influence strength and explanatory power of the expression pattern of each metabolite on the classification of each group of samples, and to mine the different metabolites with biological significance. T test was further used to verify whether the difference metabolites between groups were significant. Correlation analysis used the Pearson correlation coefficient to measure the degree of linear correlation between two metabolites.

Author contribution statement

Tongguan Tian: Performed the experiments; Analyzed and interpreted the data; Contributed reagents, materials, analysis tools or data; Wrote the paper. Yuefan Zhou : Performed the experiments. Yixin Xu: Performed the experiments. Yanping Xu: Conceived and

designed the experiments; Analyzed and interpreted the data; Wrote the paper.

Data availability statement

Data will be made available on request.

Additional information

No additional information is available for this paper.

Ethical approval

Our study was approved by the ethical committee of the Nourse Centre for Pet Nutrition.

Funding

Supported by grant from the Nourse Centre for Pet Nutrition.

Declaration of competing interest

The authors declare that they have no known competing financial interests or personal relationships that could have appeared to influence the work reported in this paper.

References

- [1] E. Biagi, C. Franceschi, S. Rampelli, M. Severgnini, Gut microbiota and extreme longevity, *Curr. Biol.* 26 (11) (2016) 1480–1485, <https://doi.org/10.1016/j.cub.2016.04.016>.
- [2] F. Kong, Y. Hua, B. Zeng, R. Ning, Gut microbiota signatures of longevity, *Curr. Biol.* 26 (18) (2016) R832–R833, <https://doi.org/10.1016/j.cub.2016.08.015>.
- [3] M.G. Rooks, S. Garrett, Gut microbiota, metabolites and host immunity, *Nat. Rev. Immunol.* 16 (6) (2016) 341–352, <https://doi.org/10.1038/nri.2016.42>.
- [4] S.R. Gill, M. Pop, R.T. Deboy, P.B. Eckburg, Metagenomic analysis of the human distal gut microbiome, *Science* 312 (5778) (2006) 1355–1359, <https://doi.org/10.1126/science.1124234>.
- [5] K. Honda, R. Littman, The microbiota in adaptive immune homeostasis and disease, *Nature* 535 (7610) (2016) 75–84, <https://doi.org/10.1038/nature18848>.
- [6] K. Atarashi, T. Tanoue, M. Ando, N. Kamada, Th17 cell induction by adhesion of microbes to intestinal epithelial cells, *Cell* 163 (2) (2015) 367–380, <https://doi.org/10.1016/j.cell.2015.08.058>.
- [7] K. Atarashi, T. Tanoue, K. Oshima, W. Suda, Treg induction by a rationally selected mixture of Clostridia strains from the human microbiota, *Nature* 500 (7461) (2013) 232–236, <https://doi.org/10.1038/nature12331>.
- [8] N. Satoh-Takayama, T. Kato, Y. Motomura, T. Kageyama, Bacteria-induced group 2 innate lymphoid cells in the stomach provide immune protection through induction of IgA, *Immunity* 52 (4) (2020) 635–649 e634, <https://doi.org/10.1016/j.immuni.2020.03.002>.
- [9] J. Hansson, N. Bosco, L. Favre, F. Raymond, Influence of gut microbiota on mouse B2 B cell ontogeny and function, *Mol. Immunol.* 48 (9–10) (2011) 1091–1101, <https://doi.org/10.1016/j.molimm.2011.02.002>.
- [10] Y. Furusawa, Y. Obata, S. Fukuda, T.A. Endo, Commensal microbe-derived butyrate induces the differentiation of colonic regulatory T cells, *Nature* 504 (7480) (2013) 446–450, <https://doi.org/10.1038/nature12721>.
- [11] C. Xu, H. Zhu, P. Qiu, Aging progression of human gut microbiota, *BMC Microbiol.* 19 (1) (2019) 236, <https://doi.org/10.1186/s12866-019-1616-2>.
- [12] M. Derrien, M.C. Collado, K. Ben-Amor, S. Salminen, W.M. de Vos, The Mucin degrader *Akkermansia muciniphila* is an abundant resident of the human intestinal tract, *Appl. Environ. Microbiol.* 74 (5) (2008) 1646–1648, <https://doi.org/10.1128/AEM.01226-07>.
- [13] M. Schneeberger, A. Everard, A.G. Gomez-Valades, S. Matamoros, *Akkermansia muciniphila* inversely correlates with the onset of inflammation, altered adipose tissue metabolism and metabolic disorders during obesity in mice, *Sci. Rep.* 5 (2015), 16643, <https://doi.org/10.1038/srep16643>.
- [14] M.N. Bouchlaka, G.D. Sckisel, M. Chen, A. Mirsoian, Aging predisposes to acute inflammatory induced pathology after tumor immunotherapy, *J. Exp. Med.* 210 (11) (2013) 2223–2237, <https://doi.org/10.1084/jem.20131219>.
- [15] M. Bodogai, J. O'Connell, K. Kim, Y. Kim, Commensal bacteria contribute to insulin resistance in aging by activating innate B1a cells, *Sci. Transl. Med.* (467) (2018) 10, <https://doi.org/10.1126/scitranslmed.aat4271>.
- [16] K. Tiihonen, A.C. Ouwehand, N. Rautonen, Human intestinal microbiota and healthy ageing, *Ageing Res. Rev.* 9 (2) (2010) 107–116, <https://doi.org/10.1016/j.arr.2009.10.004>.
- [17] F. Backhed, J. Roswall, Y. Peng, Q. Feng, Dynamics and stabilization of the human gut microbiome during the first year of life, *Cell Host Microbe* 17 (5) (2015) 690–703, <https://doi.org/10.1016/j.chom.2015.04.004>.
- [18] A. Visconti, C.I. Le Roy, F. Rosa, N. Rossi, Interplay between the human gut microbiome and host metabolism, *Nat. Commun.* 10 (1) (2019) 4505, <https://doi.org/10.1038/s41467-019-12476-z>.
- [19] Y. Lai, C.W. Liu, Y. Yang, Y.C. Hsiao, High-coverage metabolomics uncovers microbiota-driven biochemical landscape of interorgan transport and gut-brain communication in mice, *Nat. Commun.* 12 (1) (2021) 6000, <https://doi.org/10.1038/s41467-021-26209-8>.
- [20] S.M. Man, Inflammasomes in the gastrointestinal tract: infection, cancer and gut microbiota homeostasis, *Nat. Rev. Gastroenterol. Hepatol.* 15 (12) (2018) 721–737, <https://doi.org/10.1038/s41575-018-0054-1>.
- [21] S. Garde, P.K. Chodisetti, M. Reddy, Peptidoglycan, Structure, synthesis, and regulation, *EcoSal Plus* 9 (2) (2021), <https://doi.org/10.1128/ecosalplus.ESP-0010-2020>.
- [22] Y. Ke, D. Li, M. Zhao, C. Liu, Gut flora-dependent metabolite Trimethylamine-N-oxide accelerates endothelial cell senescence and vascular aging through oxidative stress, *Free Radic. Biol. Med.* 116 (2018) 88–100, <https://doi.org/10.1016/j.freeradbiomed.2018.01.007>.
- [23] L. Zheng, New insights into the interplay between intestinal flora and bile acids in inflammatory bowel disease, *World J. Clin. Cases* 10 (30) (2022) 10823–10839, <https://doi.org/10.12998/wjcc.v10.i30.10823>.
- [24] J.P. Haran, A. McCormick, Aging, frailty, and the microbiome—how dysbiosis influences human aging and disease, *Gastroenterology* 160 (2) (2021) 507–523, <https://doi.org/10.1053/j.gastro.2020.09.060>.
- [25] S. Zeng, J. Cao, Y. Chen, C. Li, Polysaccharides from *Artocarpus heterophyllus* Lam. (jackfruit) pulp improves intestinal barrier functions of high fat diet-induced obese rats, *Front. Nutr.* 9 (2022), 1035619, <https://doi.org/10.3389/fnut.2022.1035619>.

- [26] L. Philippot, B.S. Griffiths, S. Langenheder, Microbial community resilience across ecosystems and multiple disturbances, *Microbiol. Mol. Biol. Rev.* (2) (2021) 85, <https://doi.org/10.1128/MMBR.00026-20>.
- [27] S.G. Koulas, C.K. Stefanou, S.K. Stefanou, K. Tepelenis, Gut microbiota in patients with morbid obesity before and after bariatric surgery: a ten-year review study (2009-2019), *Obes. Surg.* 31 (1) (2021) 317–326, <https://doi.org/10.1007/s11695-020-05074-2>.
- [28] K. Hou, Z.X. Wu, X.Y. Chen, J.Q. Wang, Microbiota in health and diseases, *Signal Transduct. Targeted Ther.* 7 (1) (2022) 135, <https://doi.org/10.1038/s41392-022-00974-4>.
- [29] D.A. Piggott, S. Tuddenham, The gut microbiome and frailty, *Transl. Res.* 221 (2020) 23–43, <https://doi.org/10.1016/j.trsl.2020.03.012>.
- [30] M. Marizzoni, S. Provasi, A. Cattaneo, G. B. Frisoni, Microbiota and neurodegenerative diseases, *Curr. Opin. Neurol.* 30 (6) (2017) 630–638, <https://doi.org/10.1097/WCO.0000000000000496>.
- [31] J. Shen, M.S. Obin, L. Zhao, The gut microbiota, obesity and insulin resistance, *Mol. Aspect. Med.* 34 (1) (2013) 39–58, <https://doi.org/10.1016/j.mam.2012.11.001>.
- [32] M.N. Huda, M. Kim, B. J. Bennett, Modulating the microbiota as a therapeutic intervention for type 2 diabetes, *Front. Endocrinol.* (2021) 12, <https://doi.org/10.3389/fendo.2021.632335>, 632335.
- [33] W.Y. Cheng, C.Y. Wu, J. Yu, The role of gut microbiota in cancer treatment: friend or foe? *Gut* 69 (10) (2020) 1867–1876, <https://doi.org/10.1136/gutjnl-2020-321153>.
- [34] W. Zhou, Y. Cheng, P. Zhu, M.I. Nasser, Implication of gut microbiota in cardiovascular diseases, *Oxid. Med. Cell. Longev.* (2020) 2020, <https://doi.org/10.1155/2020/5394096>, 5394096.
- [35] X. Hu, T. Wang, F. Jin, Alzheimer's disease and gut microbiota, *Sci. China Life Sci.* 59 (10) (2016) 1006–1023, <https://doi.org/10.1007/s11427-016-5083-9>.
- [36] G. Bian, G.B. Gloor, A. Gong, C. Jia, The gut microbiota of healthy aged Chinese is similar to that of the healthy young, *mSphere* 2 (5) (2017), <https://doi.org/10.1128/mSphere.00327-17>.
- [37] R. Nagpal, T. Kurakawa, H. Tsuji, T. Takahashi, Evolution of gut Bifidobacterium population in healthy Japanese infants over the first three years of life: a quantitative assessment, *Sci. Rep.* 7 (1) (2017), 10097, <https://doi.org/10.1038/s41598-017-10711-5>.
- [38] F. He, A.C. Ouwehand, E. Isolauri, M. Hosoda, Differences in composition and mucosal adhesion of bifidobacteria isolated from healthy adults and healthy seniors, *Curr. Microbiol.* 43 (5) (2001) 351–354, <https://doi.org/10.1007/s002840010315>.
- [39] M. Arumugam, J. Raes, E. Pelletier, D. Le Paslier, Enterotypes of the human gut microbiome, *Nature* 473 (7346) (2011) 174–180, <https://doi.org/10.1038/nature09944>.
- [40] J.L. Fachi, J.S. Felipe, L.P. Pral, B.K. da Silva, Butyrate protects mice from Clostridium difficile-induced colitis through an HIF-1-Dependent mechanism, *Cell Rep.* 27 (3) (2019) 750–761 e757, <https://doi.org/10.1016/j.celrep.2019.03.054>.
- [41] M. Thangaraju, G.A. Cresci, K. Liu, S. Ananth, GPR109A is a G-protein-coupled receptor for the bacterial fermentation product butyrate and functions as a tumor suppressor in colon, *Cancer Res.* 69 (7) (2009) 2826–2832, <https://doi.org/10.1158/0008-5472.CAN-08-4466>.
- [42] X. Zhang, H. Yang, J. Zheng, N. Jiang, Chitosan oligosaccharides attenuate loperamide-induced constipation through regulation of gut microbiota in mice, *Carbohydr. Polym.* (2021) 253, <https://doi.org/10.1016/j.carbpol.2020.117218>, 117218.
- [43] M.E. Sanders, D.J. Merenstein, G. Reid, G.R. Gibson, R.A. Rastall, Probiotics and prebiotics in intestinal health and disease: from biology to the clinic, *Nat. Rev. Gastroenterol. Hepatol.* 16 (10) (2019) 605–616, <https://doi.org/10.1038/s41575-019-0173-3>.
- [44] P. Markowiak, K. Slizewska, Effects of probiotics, prebiotics, and synbiotics on human health, *Nutrients* 9 (9) (2017), <https://doi.org/10.3390/nu9091021>.